XAO at LBT: current performances in the visible and upcoming upgrade

Enrico Pinna[a], Fernando Pedichini[b], Simone Esposito[a], Mauro Centrone[b], Alfio Puglisi[a], Jacopo Farinato[c], Luca Carbonaro[a], Guido Agapito[a], Marco Stangalini[b], Armando Riccardi[a], Marco Xompero[a], R. Briguglio[a], Philip Hinz[d], Vanessa Bayley[d], Manny Montoya[d]

[a]INAF – Osservatorio Astrofisico di Arcetri, L.go E. Fermi 5, 50125 Firenze, Italia;
[b]INAF – Osservatorio Astronomico di Roma, Via di Frascati 33, 00040 Monte Porzio Catone, Italy;
[c]INAF - Osservatorio Astronomico di Padova, Vicolo dell'osservatorio 5, 35122 Padova, Italy;
[d]Steward Observatory, University of Arizona, 933 North Cherry Avenue, Tucson, AZ, USA

ABSTRACT

The Extreme Adaptive Optics is one of the new frontiers for astronomical AO and LBT is hosting one of the few XAO systems available on 8m class telescopes. With the 4Runner, a fast visible camera, we measured the AO performances at visible wavelengths. We were able to correct up to 500 modes at 1kHz of framerate, reaching Strehl ratios of about 40% at 630nm of wavelength. We will show the results obtained in daytime with the calibration source and on-sky using natural guidestars. These performances have been obtained at the LBTI-DX focus, one of the 4 LBT focal stations equipped with a SCAO system. All these 4 systems will be upgraded in the framework of the SOUL project. The wavefront sensor detectors will be substituted with low readout noise ones, the adaptive secondary firmware and the AO control both improved. We will briefly describe here SOUL and its performances as estimated via numerical simulations.

1. INTRODUCTION

The Large Binocular Telecope (LBT) is equipped with two Adaptive Secondary Mirrors (ASM) [1] that can work as high order Adaptive Optics (AO) correctors thanks to 672 actuators each. The ASMs are installed one for each of the two LBT eyes (DX and SX), feeding the Gregorian focal stations of the telescope. For each eye, two focal stations (LUCI and LBTI) are equipped whit a high order Pyramid WaveFront Sensor (PWFS) composing, together with the ASM, a Single Conjugated AO (SCAO) system. All the 4 systems are almost identical to the one called FLAO, described here [2]. In the second part of this work, we will show the AO performances achieved on-sky with one of these system coupled with a fast visible camera called 4Runner. The SCAO system has been pushed to its best, correcting 500 modes at 1kHz and the performances have been measured both with the 4Runner and the AO telemetry. Soon, the 4 SCAO systems will be upgraded thanks to the SOUL project. In the following session we will introduce this project and show the estimated benefits to the current SCAO systems of LBT.

2. SOUL: UPGRADING THE LBT SCAO SYSTEMS

2.1 SOUL in brief

SOUL is the upgrade for the 4 single conjugated AO systems of LBT, namely the two FLAO at the LUCI1 and LUCI2 foci and the two LBTIAO serving the LBTI instruments. The core of the upgrade is the implementation of a new generation visible detector for the wavefront sensing, allowing higher SNR and higher sampling both in the temporal and spatial domain. The higher temporal sampling of the camera will be matched by the Adaptive Secondary Mirror (ASM) thanks to a firmware upgrade, so that, the upgraded AO system will get a performance and robustness gain.

The SOUL project is currently in its preliminary design phase. In the first phase of this study, we performed an error budget computation, comparing different suitable WFS detectors available on the market and evaluating their performances in terms of AO residuals. This analysis leads us to the selection of the OCAM2k as new WFS detector.

This camera has an Electron Multiplied CCD chip (E2V CCD220) and provides a very high framerate (2kHz) with a very low RON (0.37e^-). In Table 1 we compare the main features of the current WFS camera (CCD39 by Sciemeasure) and the OCAM2k by First Light. The error budget analysis, considering both bright and faint guide stars, showed 40SA (Sub-Apertures) across the pupil as best compromise between maximum contrast and sky coverage for the maximum pupil sampling with OCAM2k. This sampling can be reduced accordingly with the star flux to 20, 13.3 and 10SA binning the CCD by 2x2, 3x3 and 4x4 respectively.

Table 1. The main characteristics of the current (CCD39) and new (OCAM2k) WFS detectors.

Spec/camera	CCD39	OCAM2k
Chip size [pix]	80x80	240x240
Pixel side [μm]	24	24
RON [e-]	10.5 (1kfps)	0.37 (2kfps, G=400)
Excess noise	NO	$\sqrt{2}$
Max. framerate [fps]	1000	3625 (ROI 120x120)
Min. read-out time [ms]	0.95	0.24 (ROI 120x120)

2.2 SOUL Error Budget

The error budget model we considered in the SOUL design study takes into account the following terms:

- Closed loop rejection transfer function (A)
- Closed loop noise transfer function (A)
- Temporal error (A)
- Fitting error (A)
- WFS Noise Propagation coefficients (N)
- Pyramid optical gain in partial correction regime (N)
- Aliasing (N)

where the terms marked with "A" are represented by an analytical model, while those marked with "D" are taken into account numerically[1].

As a first step we optimized the AO parameters for each of the considered reference star magnitude (7.5<R<18.5 at 1 magnitude step). The considered parameters are: detector binning (pupil sampling), number or corrected modes and loop framerate, loop integrator gain (here a single value is considered for all modes). We performed this optimization for both CCD39 and OCAM2k cases, considering a seeing of 0.8", L_0=40m and a wind speed of 16m/s. Exploring the complete parameter space, we identified the best configuration as the one providing the lower wavefront residuals. We report the obtained results in Figure 1. The wavefront residuals represent the performance estimation that we translated into SRs values using the Maréchal's approximation. The plots of the obtained SRs at 3 different wavelengths are reported in Figure 2. The comparison between the error budget of the current SCAO system (CCD39) and the one upgraded with

[1]These terms have been computed by means of end-to-end simulations with the PASSATA software.

SOUL (OCAM2k) shows a gain of 1 to 2 magnitudes of reference star for the same achieved wavefront correction. This represents a dramatic improvement in terms of sky coverage at all wavelengths.

CCD39 – 30x30 SAs

GS Rmag	CCD bin	Loop freq [Hz]	Corrected modes	gain	WF RMS [nm]
7.5	1	1000	663	0.55	91.8
8.5	1	1000	663	0.50	95.3
9.5	1	400	634	1.00	107.2
10.5	1	300	443	1.40	123.5
11.5	1	300	331	1.10	159.4
12.5	2	300	147	1.10	185.0
13.5	2	200	145	1.40	213.0
14.5	3	200	77	1.00	286.2
15.5	3	100	58	1.50	362.9
16.5	3	50	54	1.80	460.9
17.5	4	50	34	1.20	631.5
18.5	4	50	11	0.70	897.3

OCAM2k – 40x40 SAs

GS Rmag	CCD bin	Loop freq [Hz]	Corrected modes	gain	WF RMS [nm]
7.5	1	2000	663	0.40	82.9
8.5	1	2000	663	0.40	84.7
9.5	1	2000	663	0.30	88.3
10.5	1	1800	663	0.30	96.0
11.5	1	500	633	0.90	112.3
12.5	1	400	471	1.00	134.1
13.5	1	300	312	1.20	170.4
14.5	2	300	196	0.80	218.2
15.5	3	200	90	1.00	290.3
16.5	4	200	54	0.70	374.5
17.5	4	100	54	0.90	463.3
18.5	4	50	48	1.20	636.7

Figure 1. The table on the left reports the AO parameters optimized for different guide-star magnitudes for the current system implementing the CCD39 and a pupil sampling of 30SA across the diameter. The last column reports the estimated wavefront residual. The table on the right reports the same quantities for the case of the system upgraded with the OCAM2k and a pupil sampling of 40SA.

The error budget analysis provides the overall wavefront residual together with its distribution in the considered error terms. In Figure 3 we report a bar diagram with the distribution at each considered star magnitudes. In the bottom part of the same figure, we report a schematic with the main parameters. We can see that, at high flux, SOUL improves mainly the time (faster framerate and low read out time) and aliasing errors (pupil oversampling), while the absolute value of the fitting error is constant (limited by the degrees of freedom of the corrector). Moving to fainter fluxes, the low RON of OCAM2k allows to keep higher framerates and pupil sampling, improving all the error budget terms.

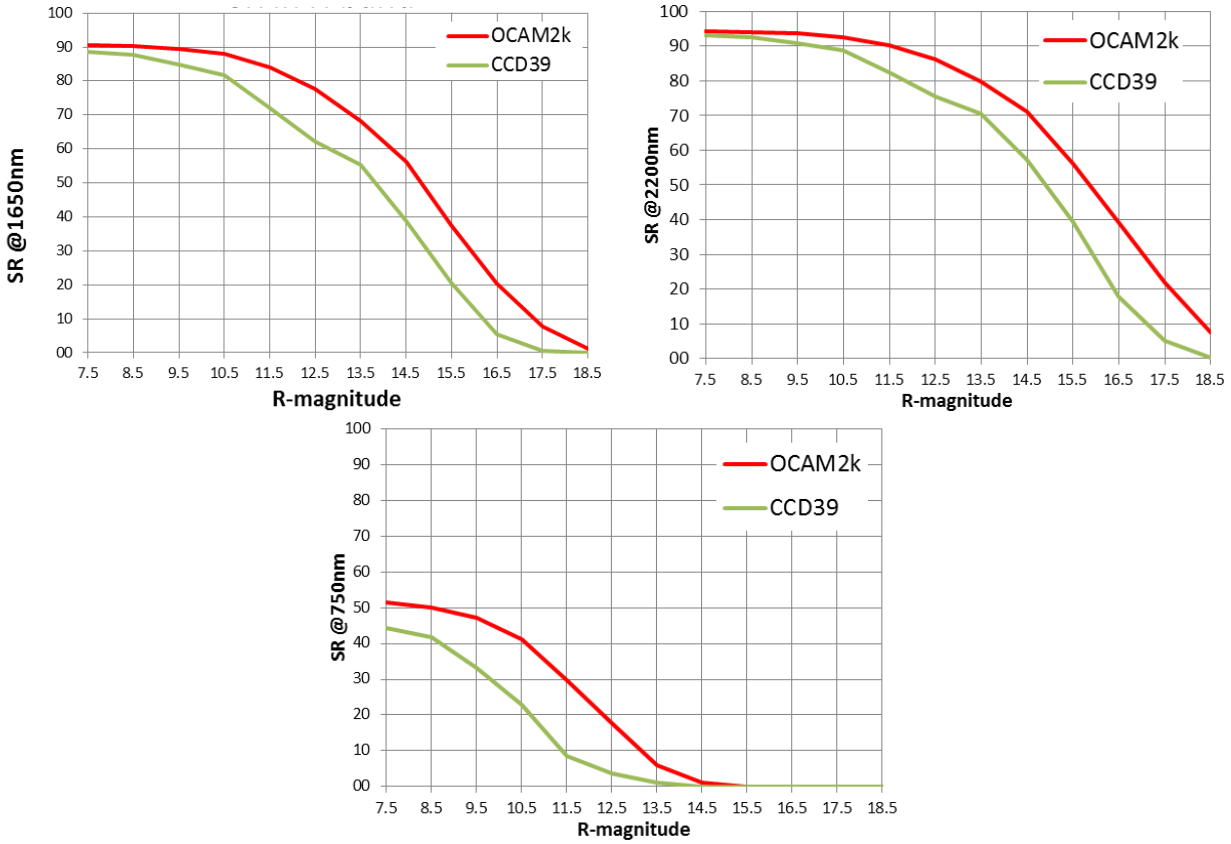

Figure 2. The estimated performances of the AO system in term of SR as function of the reference star magnitude and at different wavelengths. The green line shows the values for the current system and the red one for the one upgraded in the SOUL project.

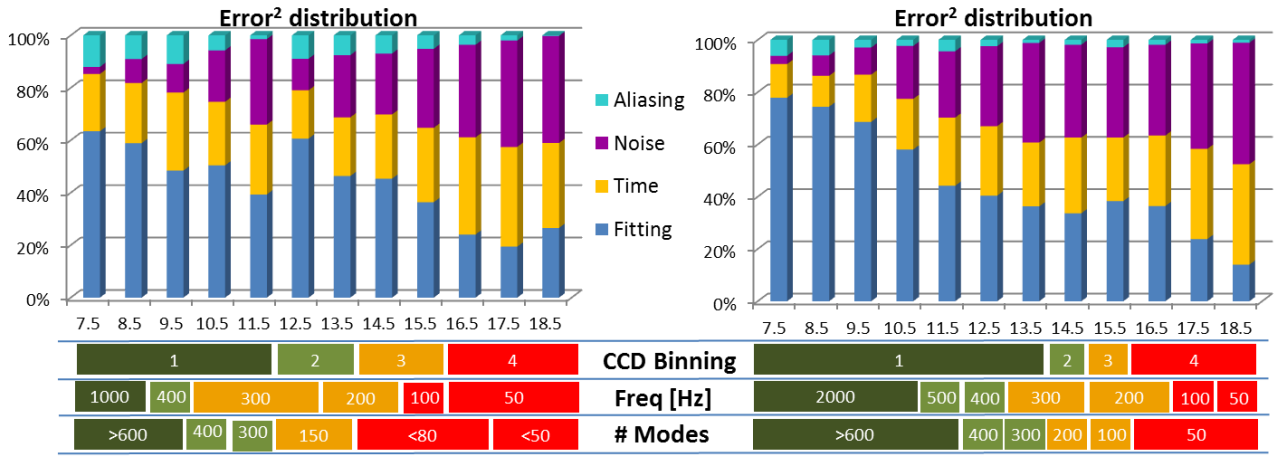

Figure 3. Top: the bar diagram shows the distribution of the error terms before (left) and after (right) the upgrade at different guide star magnitude (horizontal axis). Bottom: schematic representation of the optimized AO parameter at the different guide star magnitudes.

3. AO PERFORMANCES WITH THE SHARK 4RUNNER

3.1 The 4Runner

Recently we had the first measurement on sky of the SCAO performances at visible wavelengths with the 4Runner. The 4Runner is the demonstrator for the LBT next generation instrument called V_SHARK [4]. This instrument is a high contrast imager and coronagraph in the band 0.6-0.9μm; a similar instrument (SHARK-NIR [5]), working in the NIR, will be installed on the other LBT eye and it will be matched with its counterpart . All the detail about V_SHARK and 4Runner can be found in [4], while in this section we will provide just a brief description of the 4Runner's hardware in order to give a general picture of the setup used for the measurement described below. The 4Runner consist in a pick-up deployable arm and a board housing a fast visible camera (Andor Zyla) featuring a framerate of 1kHz (on a 200x200pix ROI) with a very low RON ($1e^-$). Just in front of the camera we placed a lens, adjusting the pixelscale to 3.8mas/pix and a colored filter centered on 630nm with a bandwidth of 40nm. In Figure 4 we report a sketch of the optical scheme. The star light coming from the adaptive secondary is reflected by the tertiary mirror toward the LBT focal station. When the 4Runner arm is deployed, a visible beam splitter and a folding mirror redirect half of the incoming flux toward the fast camera. The remaining 50% of the light follows its original path reflected by the LBTI dichroic toward the AO WFS. A picture of the hardware installed on the telescope is reported in Figure 5.

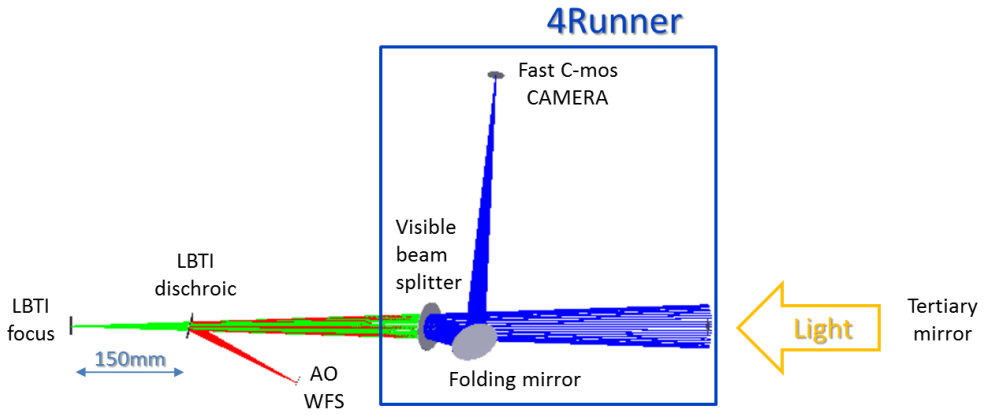

Figure 4. Zemax layout of the 4Runner's optical configuration.

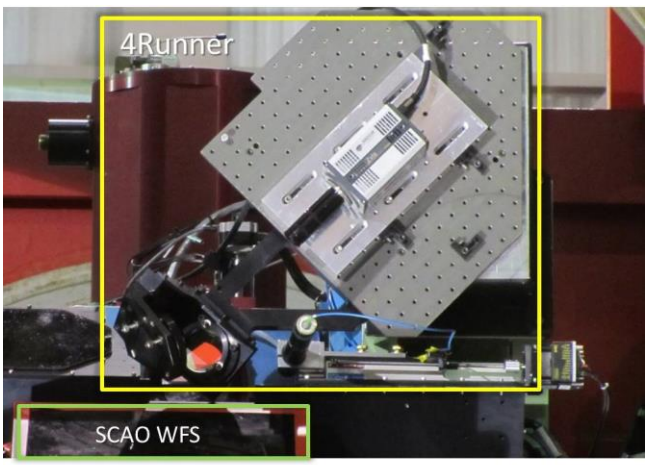

Figure 5. Picture of the 4Runner (yellow square) installed at the LBTI-DX focal station with its pick-up arm deployed. The green square shows the position of the AO WFS.

3.2 On-sky performances

Before the on-sky test, we calibrated the AO system, acquiring a new interaction matrix and correcting for the Non-Common-Path Aberrations (NCPA). The new AO calibration provided a reconstruction matrix working properly with 500 modes; the NCPA showed to be dominated by 30nm of astigmatism introduced, as expected by design, by the beam splitter of the 4Runner pick-up arm. We successfully compensated the measured NCPA offsetting the AO loop working point, as described in [1].

During the night test, we closed the loop on a few bright stars in order to measure the AO performance with the 4Runner. Here we report the data we obtained using an R=6 star, during its transit close to zenith (elevation=84deg). The seeing was estimated by the LBT DIMM 20min before the data acquisition to be around 1.0". During the data acquisition the DIMM was not available. The AO system was running at a framerate of 990Hz and providing telemetry data with a decimation of 3, corresponding to a framerate of 330Hz. From the vectors s (WFS slopes) and p (mirror positions) we can estimate the residual wavefront and the correction applied by the AO system. We can get the residual wavefront expressed in vector of modal amplitudes as $m_R = s \cdot \boldsymbol{R}$; where $\boldsymbol{R}$ is the reconstruction matrix obtained from the interaction matrix measured in diffraction limited conditions. We know that the pyramid wavefront sensor varies its sensitivity when is working in partial correction conditions. This is taken in to account rescaling the slopes: $s = s_M / G_{OPT}$; where s_M are the slope values measured by the pyramid WFS and G_{OPT} is the optical gain compensation measured on-sky as fully described in [1]. The G_{OPT} factor is here the key in order to have the m_R vector properly scaled. The used modal basis is ortho-normalized, so we can estimate the total residual wavefront w_R at each loop step i as: $w_R(i) = \sqrt{\sum_{n=0}^{500} m_R^2(n,i)}$, where n is the modal index. From the same vector we can also estimate the residual tip-tilt free wavefront as $w_{RTT}(i) = \sqrt{\sum_{n=2}^{500} m_R^2(n,i)}$. Of course, we should add to these values the contribution of the fitting error associated to our modal basis that we are using for the wavefront reconstruction. We can estimate this quantity with the expression $\sigma_{fit}^2 = 0.2778 N^{-0.9} \left(\frac{D}{r_0}\right)^{5/3}$, as reported in [6]. For seeing values around 1.0" we get an estimated fitting error of about 75nm. Because this value is highly dependent on the seeing and its value it is not known reliably, we prefer to not include it in the wavefront residual and keep considering just $w_R(i)$ and $w_{RTT}(i)$ as defined before.

We estimate the correction applied by the AO system thanks to the vector $p(i)$, composed by the measurement of the capacitive sensor of each ASM's actuator. We can represent our modal basis as a Matrix ***M2C***, giving the position of each ASM actuator for each mode. We used $\boldsymbol{C2M} = \boldsymbol{M2C}^{-1}$ to obtain the modal amplitudes $m_C(i) = C2M\, p(i)$ and compute the amount of applied correction at each loop step as $w_C(i) = \sqrt{\sum_{n=0}^{500} m_C^2(n,i)}$. In Figure 6 we report the temporal behavior of the 3 quantities (w_R, w_{RTT}, w_C) in a window of 2.5s.

In order to estimate the modal distribution of the applied correction and residuals, we report in Figure 7 the standard deviation (over 4s) of the vectors w_R and w_C. The plots confirm that the loop is effectively correcting all the 500 considered modes. We can notice a small jump in the wavefront residuals around mode 120. This jump can be explained as a feature of the integrator gain optimization. The integrator gain value is found on-sky at the beginning of closed loop operations and its value is optimized for the each of the 3 groups of modes: tip-tilt, modes 3-119, modes 120-500.

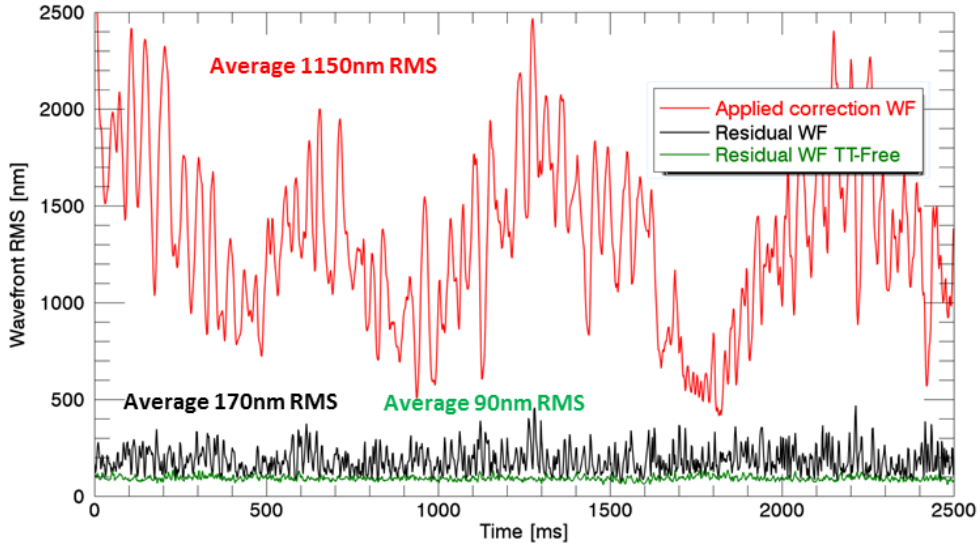

Figure 6. The plot represents the temporal behavior of the applied correction (red), the residual (black) wavefront error estimated by the WFS and the same value without considering the tip-tilt residuals. These values are computed from on-sky measurement as described in the body text.

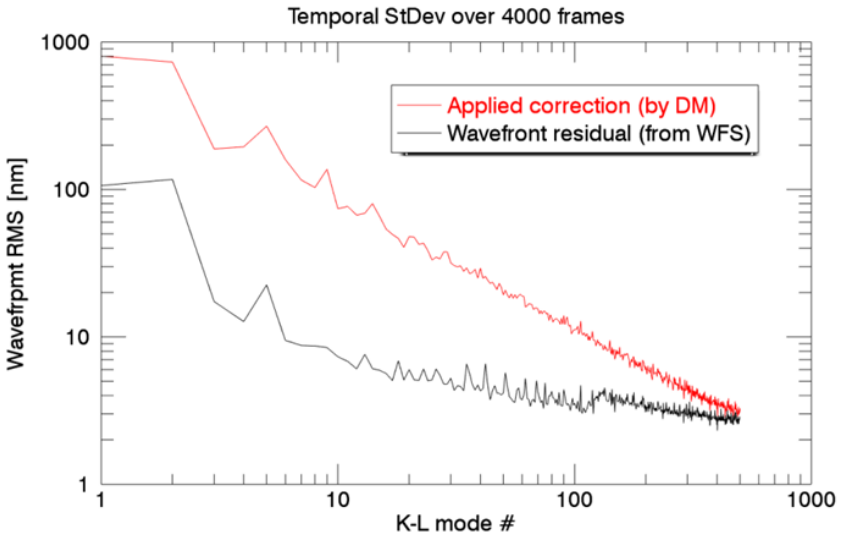

Figure 7. The plot shows the standard deviation in time of the correction applied (red) and the wavefront residual (black) for each of the 500 corrected modes.

The PSF recorder on the 4Runner during the closed loop is reported in Figure 8. This image is obtained from 1000 exposures of 1ms each, shifted and then averaged. This PSF shows a SR of about 40% and a full width half maximum of 19mas. In Figure 9 we can see the radial profile of this image, normalized to its SR and compared with theoretical diffraction limited PSF. In both Figure 8 and Figure 9 we can see the AO control radius at about 230mas off-axis, preceded by a high contrast region, where several diffraction rings are clearly visible.

The shown PSF is a typical result obtained during this night test at LBT and reduced with the 4Runner's automatic procedure. More data of the same night, treated with a more sophisticated data reduction, show even higher SRs and better contrasts, as reported in [3].

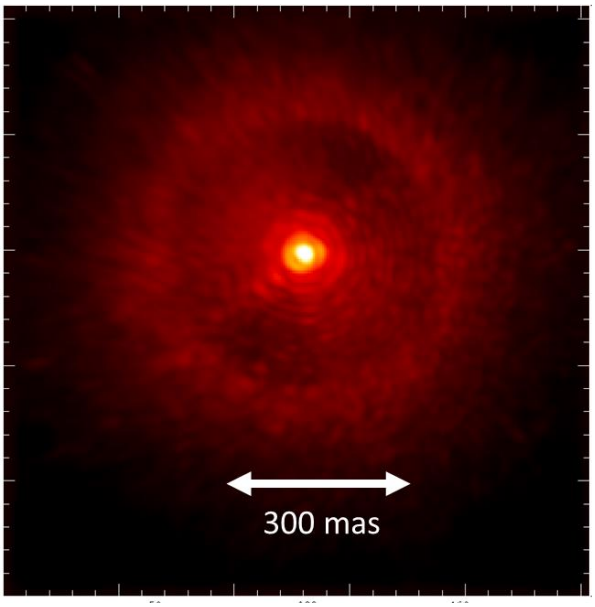

Figure 8. A log display of the guide star image acquired at 630nm during the AO correction. The image is obtained by shift and add of 1000 frames of 1ms each.

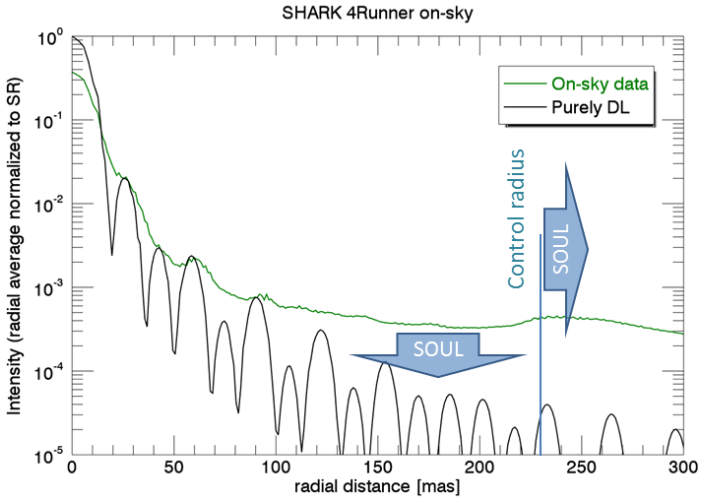

Figure 9. The radial profile of the on-sky PSF reported in Figure 8 (green). The intensity is normalized to its SR value in order to allow the comparison with the diffraction limited profile (black). The two blue arrows shows graphically the benefits that SOUL will bring to the PSF profile in bright regime, increasing the number of corrected modes (pushing the control radius further off-axis) and improving the contrast thanks to the reduced aliasing and time errors.

4. CONCLUSION

We reported here the on-sky results obtained in June 2015 with one of the SCAO system coupled with the SHARK 4Runner. These results demonstrate that the current system is able to correct the wavefront using 500 modes at about 1kHz, providing SRs of the order of 40% and high contrast (10^{-3}) even at visible wavelengths (630nm). These

performances are encouraging the development of optical high contrast instruments as SHARK-NIR and V_SHARK, the last one following the path opened by the MagAO system [7]. Moreover, we presented here the performance improvement expected on the LBT SCAO systems after the upgrade foreseen in the SOUL project. The new generation WFS detector will allow to improve the AO performances in all the range of reference star magnitudes. We quantified this benefit in a gain in between 1 and 2 guide star magnitudes. The SOUL project is currently in preliminary design phase and it is foreseen to have the first light in 2017. The upgraded SCAO systems will feed the existing instruments LUCI1-2 and LBTI, and, in the next future, the V_SHARK and SHARK-NIR, foreseen at the telescope both in 2018.

5. ACKNOWLEDGMENTS

The 4Runner team wants to thank all the LBTO personnel for the support given to the 4Runner project. This help has been crucial to make this test happen in all its phases: the telescope time, the logistic for the hardware transportation and finally the collaboration of the telescope crew during the operations.

REFERENCES

[1] Riccardi, A, et al., "The adaptive secondary mirror for the Large Binocular Telescope: optical acceptance test and preliminary on-sky commissioning results," Proceedings of the SPIE, Volume 7736 (2010)
[2] Esposito, S., et al., "First light AO (FLAO) system for LBT: final integration, acceptance test in Europe, and preliminary on-sky commissioning results," Proceedings of the SPIE, Volume 7736 (2010)
[3] Esposito, S., et al.,"Non common path aberration correction with nonlinear WFSs," Proceedings of AO4ELT4 (2015).
[4] Pedichini, F., et al.,"The Visible channel of SHARK and the 4runner experiment," Proceedings of AO4ELT4 (2015).
[5] Farinato, J., et al., "SHARK-NIR Channel: an high contrast imager with coronographic capabilities for the Large Binocular Telescope," Proceedings of AO4ELT4 (2015).
[6] Quiros-Pacheco, F., et al.,"First light AO (FLAO) system for LBT: performance analysis and optimization," Proceedings of SPIE Volume 7736 (2010).
[7] Males, J, et al., "Imaging exoplanets at visible wavelengths from the ground," Proceedings of AO4ELT4 (2015).